



A Journal of the Gesellschaft Deutscher Chemiker

Angewandte Chemie

GDCh

International Edition

www.angewandte.org

Accepted Article

Title: Multiexcitonic Triplet Pair Generation in Oligoacene Dendrimers as Amorphous Solid-state Miniatures

Authors: Juno Kim, Hao Ting Teo, Yongseok Hong, Juwon Oh, Hyungjun Kim, Chunyan Chi, and Dongho Kim

This manuscript has been accepted after peer review and appears as an Accepted Article online prior to editing, proofing, and formal publication of the final Version of Record (VoR). This work is currently citable by using the Digital Object Identifier (DOI) given below. The VoR will be published online in Early View as soon as possible and may be different to this Accepted Article as a result of editing. Readers should obtain the VoR from the journal website shown below when it is published to ensure accuracy of information. The authors are responsible for the content of this Accepted Article.

To be cited as: *Angew. Chem. Int. Ed.* 10.1002/anie.202008533

Link to VoR: <https://doi.org/10.1002/anie.202008533>

RESEARCH ARTICLE

Multiexcitonic Triplet Pair Generation in Oligoacene Dendrimers as Amorphous Solid-state Miniatures

Juno Kim,^{[a],†} Hao Ting Teo,^{[b],†} Yongseok Hong,^[a] Juwon Oh,^[a] Hyungjun Kim,^{*,[c]} Chunyan Chi,^{*,[b]} and Dongho Kim^{*,[a]}

Abstract: Singlet fission in organic semiconducting materials has attracted great attention for the potential application in photovoltaic devices as the exciton multiplication process effectively compensates for thermal energy losses. Research interests have been concentrated on identifying working mechanisms of coherent SF processes in crystalline solids as ultrafast SF is hailed for efficient multiexciton generation. However, as long lifetime of the intermediate state, multiexcitonic triplet pair, in amorphous solids facilitates the decorrelation process for triplet exciton extractions, a precise examination of incoherent SF processes is demanded in delicate model systems to represent heterogeneous structures. By introducing dendritic structures, heterogeneous coupling and energetics for SF were developed in our oligoacene oligomers, which mimic complicated SF dynamics in amorphous solids. SF dynamics in dendritic structures was thoroughly investigated by time-resolved spectroscopic techniques and quantum chemical calculations in respect of the relative orientation/distance between chromophores and through-bond/-space interactions.

Introduction

In a recent decade, singlet exciton fission (SF) process which generates multiexcitonic triplet pair in organic semiconducting materials has attracted great attention since the exciton multiplication process converting a singlet exciton into two triplets effectively compensates for thermal energy losses.^[1-10] Recently, Einzinger et al. presented a successful report on the sensitization of the silicon solar cell by triplet excitons generated via SF process in the tetracene layer, which envisions the prospect to surpass the upper bound of the cell efficiency determined by the Shockley-Queisser limit of 33%.^[11-13] By introducing a hafnium oxynitride interlayer which lies between the silicon and tetracene layers, triplet excitons generated via SF processes in the tetracene layer were efficiently transferred with the combined yield of 133% which includes SF and triplet energy transfer

processes. In a cooperative manner to employ SF process in photovoltaic devices, a precise control of microscopic morphology of SF active layer for efficient SF processes and triplet exciton extractions is raised to boost up the solar cell efficiency up to 45.9%, in parallel with devising optimal cell structures.^[14-15]

SF processes in organic systems can be divided into two broad categories of coupling regimes by coherent and incoherent mechanisms. Coherent SF processes are facilitated by the configuration mixing between local excitonic states and multiexcitonic triplet pair states, which is strengthened in π - π stacked structures such as slip-stacked conformations via effective orbital interactions.^[16-17] SF processes in the incoherent coupling regime proceed in weakly coupled systems whose orbital interactions are weak or the energetic proximity of local exciton with the intermediate, multiexcitonic triplet pair, is poor.^[18] For coherent SF processes, the intervention of virtual charge transfer states, direct and vibronic coupling mechanisms have been proposed to account for ultrafast SF dynamics in crystalline solids by numerous previous reports.^[19-35] However, incoherent coupling regimes in amorphous solids have been a relatively inactive research area since coherent SF pathways are hailed as much efficient channels for multiexcitonic triplet pair generation.^[36-40] Recently, the decorrelation and separation of multiexcitonic triplet pairs into individual triplet excitons were reported to be much facilitated in amorphous solids prepared by pristine SF molecules or covalently linked SF oligomers whose SF processes proceed in incoherent regimes.^[41] Unlike previous viewpoints on SF efficiency, achieving long lifetime of the multiexcitonic triplet pairs is regarded important for their spatial separation process to extract doubled triplet excitons, which raises the importance of understanding incoherent coupling regimes.

In the meantime, incoherent SF processes have been mostly examined in molecular dimers by changing linkage types between two chromophores to control relative orientations.^[42-53] Feng et al. and Ito et al. evaluated incoherent SF processes partitioning couplings into direct-overlap and bridge-mediated contributions in such molecular dimers based on quantum chemical simulations.^[54-56] These works provided the importance of both the relative orientation and distance between chromophores and the contribution of through-bond and space interactions in incoherent coupling regimes. However, such molecular dimers do not reflect the characteristic feature of amorphous solid-states, a structural heterogeneity, which complicates electronic coupling and energetic landscape. In this regard, molecular oligomers (trimer, tetramer and hexamer conformations) were prepared in several forms of dendrimers to mimic heterogeneous structures present in amorphous solids. Each type of two chromophores, 6,13-bis(triisopropylsilylethynyl)pentacene (TIPS-pentacene) and 5,12-bis(triisopropylsilylethynyl)tetracene (TIPS-tetracene), was attached to a core phenyl unit controlling the number of chromophores and linking positions as depicted in Figure 1. Our

J. Kim [†], Y. Hong, Dr. J. Oh, Prof. Dr. D. Kim
Department of Chemistry
Spectroscopy Laboratory for Functional π -Electronic Systems
Yonsei University
03722, Seoul (Korea)
E-mail: dongho@yonsei.ac.kr

H. T. Teo [†], Prof. Dr. C. Chi
Department of Chemistry, National University of Singapore
3 Science Drive 3, 117543 Singapore (Singapore)
E-mail: chmcc@nus.edu.sg

Prof. Dr. H. Kim
Department of Chemistry, Incheon National University
22012, Incheon (Korea)
E-mail: kim.hyungjun@inu.ac.kr

[†]: This mark denotes J. Kim and H. T. Teo are co-first authors.

RESEARCH ARTICLE

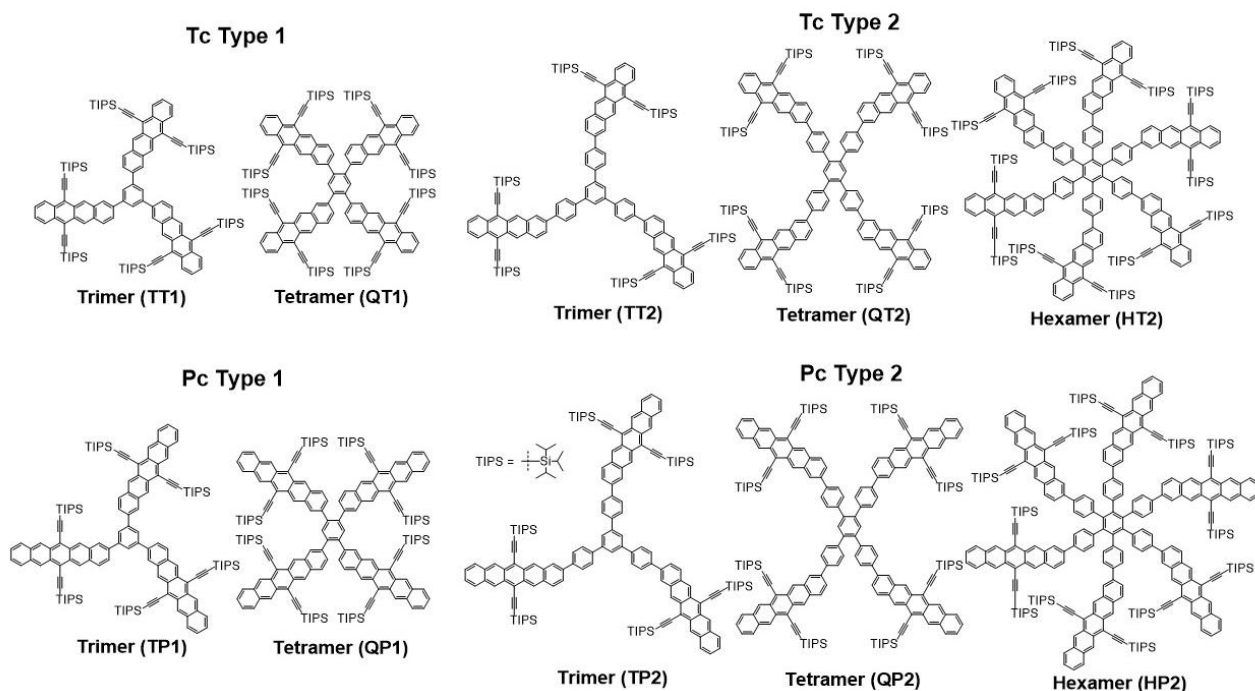


Figure 1. Molecular structures of Type1 (left) and Type2 (right) oligoacene dendrimers composed of TIPS-tetracene (top) and TIPS-pentacene (bottom).

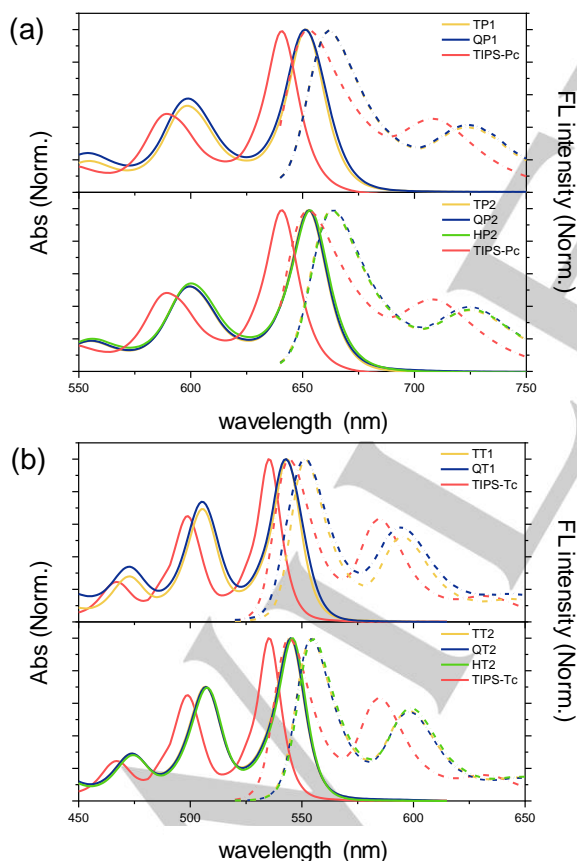


Figure 2. Steady-state absorption (solid lines) and fluorescence spectra (dashed lines) of TIPS-pentacene dendrimers (a) and TIPS-tetracene dendrimers (b) recorded in toluene. Top and bottom panel of each figure contain Type1 and Type2 chromophores, respectively.

weakly interacting dendritic structures are divided into two groups, Type1 and Type2 dendrimers, depending on whether oligoacene units are directly bonded to the core or an additional phenyl moiety is substituted to each unit. The synthesis and characterization of these dendrimers are described in supporting information (SI). The effects of chromophore multiplications and heterogeneous couplings for SF processes were thoroughly investigated in our amorphous solid-state miniatures on the basis of transient absorption, time-resolved fluorescence spectroscopies and theoretical calculations.

Results and Discussion

Steady-state measurements

The steady-state absorption and fluorescence spectra of TIPS-tetracene and TIPS-pentacene dendrimers were recorded in toluene (Figure 2). The absorption spectra reflect interactions between chromophores within each dendritic structure in the ground-state. As absorption peaks are independent of the number of oligoacene constituents and the type of dendrimers (Type1 and Type2), weak interactions between oligoacene units are suggested in both Type1 and Type2 dendrimers. Compared to TIPS-tetracene and TIPS-pentacene monomers, only slight changes in 0-0 to 0-1 peak ratios and red-shifts of absorption peaks are shown for dendrimers, which originates from the electronic perturbation on the aromatic backbone of oligoacenes by end-substitution with a phenyl unit.^[44, 57] Likewise, their fluorescence spectra are red-shifted compared to the monomers while peak positions are maintained regardless of the number of oligoacene constituents and the type of dendrimers. It is

RESEARCH ARTICLE

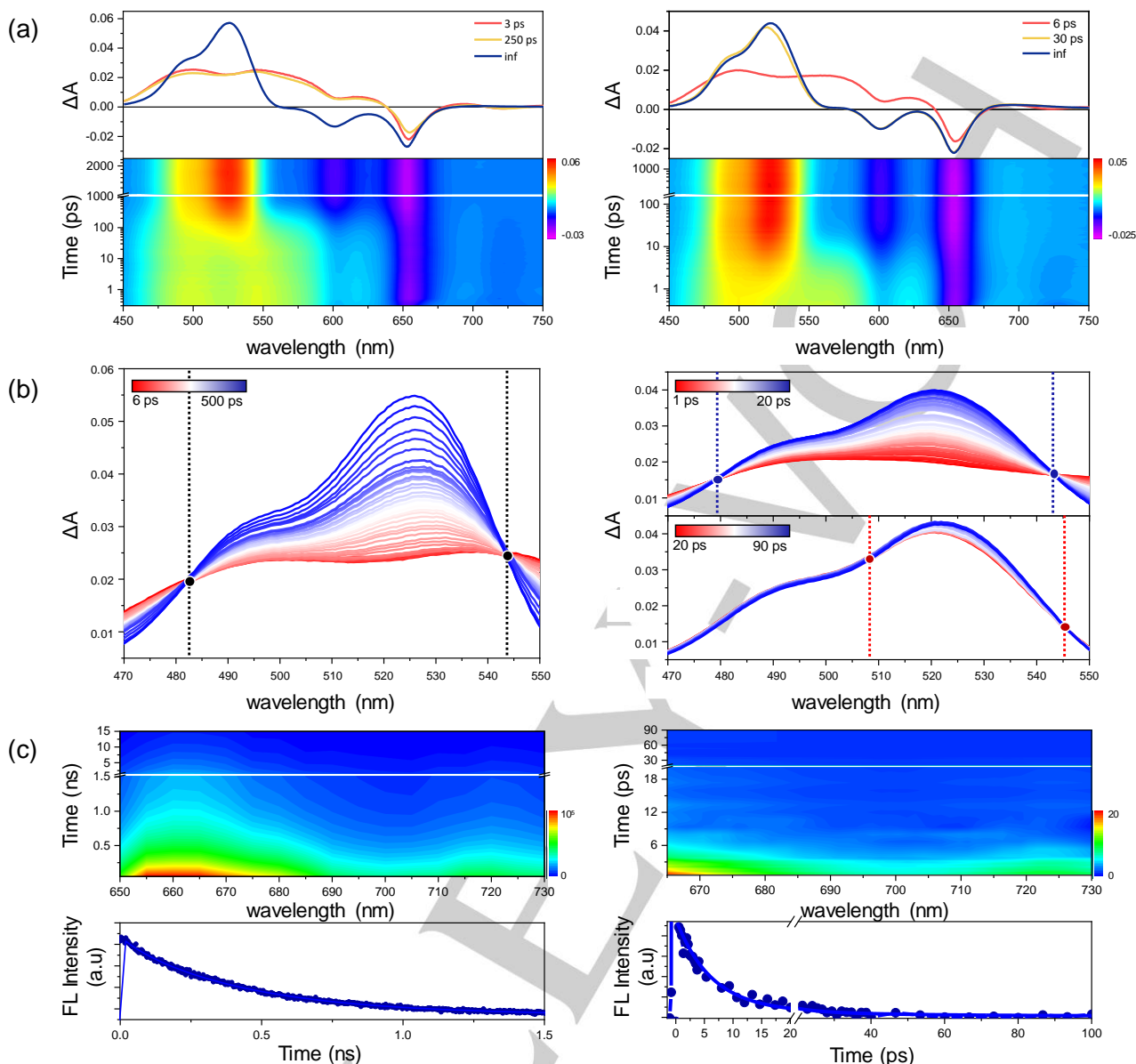


Figure 3. (a) Species associated spectra (SAS) (top) and 2D contour maps (bottom) obtained from *fs*-transient absorption measurements in toluene for **TP1** (left) and **QP1** (right). SAS are analysed by GloTarAn program.^[75] (b) Isosbestic points (dashed lines) shown from magnified *fs*-transient absorption spectra of **TP1** (left) and **QP1** (right). (c) 2D contour maps (top) and decay profiles (bottom) of time-resolved fluorescence in toluene for **TP1** (left) and **QP1** (right) recorded by time-correlated singlet photon counting and broadband fluorescence upconversion techniques.

noteworthy that their fluorescence spectra are close to the mirror image of absorption spectra, which excludes the configuration mixing of emissive local excitonic states with charge resonance and multiexcitonic triplet pair states. Weak electronic interactions in the excited states imply incoherent coupling regimes for possible SF processes in the dendrimers. The steady-state absorption and fluorescence spectra were further investigated under polar environments such as tetrahydrofuran (Figure S45). Besides the effect from changes in refractive index, their steady-state properties are scarcely modulated in tetrahydrofuran medium. Negligible red-edge tail bands in the absorption spectra and well-defined vibronic structures in the fluorescence spectra exclude contributions of charge transfer interactions and configuration mixings even in the polar medium.^[58-59] In addition, charge-transfer (CT) states are

monitored energetically high above the local excitonic state by our quantum chemical calculations (Table S4-S36), which may exclude CT-mediated SF mechanism unlike previous reports.^[27, 34-35, 50, 52, 60-62] As oligoacene units are symmetrically substituted at their 6 and 13 positions by TIPS groups, we assume charge-transfer mediation in SF dynamics may not be operative for the dendrimers, unlike charge-transfer mediated SF processes in pentacene dimers whose substituent and linker are bonded asymmetrically at their 6 and 13 positions, respectively.^[50, 52] In this respect, the dendrimers prepared here are exemplary molecular systems for investigating couplings between two pure quantum states, the local excitonic and multiexcitonic triplet pair state, with regard to microscopic structures.

RESEARCH ARTICLE

Time-resolved spectroscopic measurements

To investigate SF processes, *fs*-transient absorption and time-resolved fluorescence measurements were conducted in toluene for the dendrimers (Figure 3 and S46-S65). Observations from time-resolved measurements on TIPS-pentacene dendrimers are described dividing them into Type1 trimer/tetramer (**TP1/QP1**), Type2 trimer/tetramer (**TP2/QP2**) and Type2 hexamer (**HP2**). For **TP1** and **QP1**, multiexcitonic triplet pair generation was investigated in terms of the linking positions of pentacene units in each dendrimer. By comparing Type1 and Type2 trimers/tetramers, the role of additional phenyl linkers is explicitly shown. For **HP2**, an unexpected channel for fast multiexcitonic triplet pair generation is suggested, which contrasts with observations from **TP2** and **QP2**. SF processes in TIPS-tetracene dendrimers are covered in the supplementary note in SI.

For **TP1** and **QP1**, broad excited-state absorption (ESA) bands of S_1 state spanning from 450 to 630 nm region are shown at the initial time delay of *fs*-transient absorption (TA) spectra. Along with decay dynamics of S_1 state, rise of distinct ESA bands around 520 nm and ground-state bleaching (GSB) around 660 nm was shown as the typical spectral evolution driven by SF process in pentacene systems.^[23-25, 28, 42, 44, 48, 50, 52] However, it is noteworthy that GSB bands do not rise along with SF dynamics in the series of *para*-phenylene-bridged pentacene dimers (**BPO** and **BP1**) whose conjugation between chromophores is extensive as revealed by DFT calculations.^[44] Unlike *para*-phenylene-bridged pentacene dimers, each chromophore within **TP1** is substituted at *meta*-position where the electronic interaction is much weaker compared to that at *ortho*- and *para*-positions.^[63] Besides, chromophores within **QP1** are orthogonal to the core phenyl group due to steric hindrance, which deteriorates conjugation effects. Due to structural dissimilarities, interactions between TIPS-pentacene units are relatively much weaker in the dendrimers, which accounts for the rise of GSB bands around 650 nm in *fs*-transient absorption spectra. While **TP1** and **QP1** share the similar spectral evolution illustrated above as SF processes proceed, there exists a clear difference in SF kinetics. The SF process in **TP1** proceeds at the rate of 250 ps, however, the generation of multiexcitonic triplet pair in **QP1** is biexponential exhibiting time constants of 6 and 30 ps. As depicted in Figure 3, two pairs of isosbestic points are found from *fs*-transient absorption spectra of **QP1** along with biphasic spectral rises of triplet state ESA around 520-525 nm. Simply, the relatively faster SF process in **QP1** is well accounted for by the proximity between chromophores linked at *ortho*-positions, which enhances electronic coupling. However, the mechanism of biexponential SF in **QP1** should be further understood. Recently, Lee et al. reported biexponential SF dynamics in polycrystalline films of TIPS-pentacene employing temperature-dependent transient absorption measurements.^[64] The second process followed by multiexcitonic triplet pair generation was described as a triplet energy transfer process, which develops loosely bound triplet pair. In another report, a relatively slower component of SF processes was regarded as the energy transfer process of bright excitons (S_1) to optimal spots for SF process within heterogeneous solid films.^[45] So far, however, biphasic SF processes in the solution phase have not been thoroughly demonstrated. To attain further insights into the biexponential SF dynamics in **QP1**, time-resolved

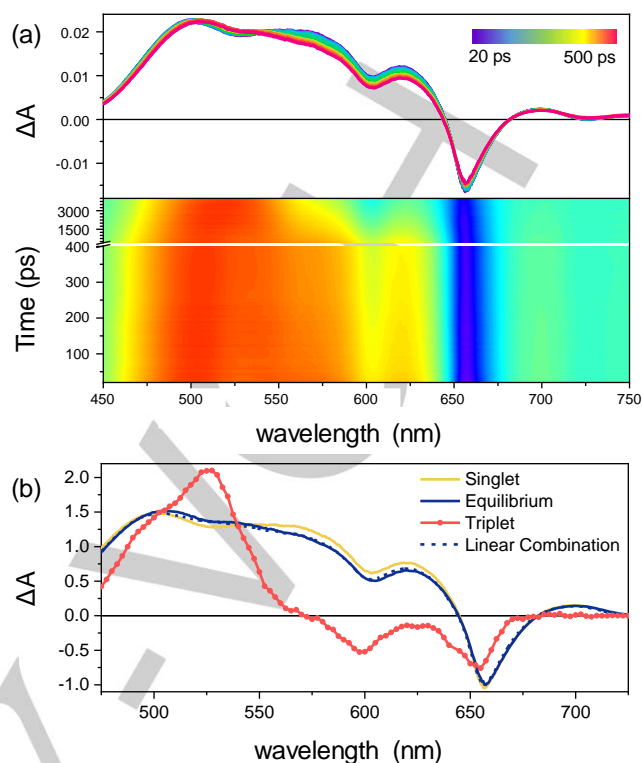


Figure 4. (a) The *fs*-transient absorption spectra (top) and 2D contour map of **HP2** in toluene. (b) Spectrum of **HP2** obtained from global analysis (equilibrium) overlaid with the linear combination of singlet and triplet spectra. Triplet spectrum obtained from *ns*-TA measurements (2.5 nm wavelength interval) is linearly interpolated for the linear combination.

fluorescence measurements were conducted as shown in Figure 3. In line with *fs*-transient absorption measurements, biexponential decays of fluorescence intensity were monitored as excited-state populations are transferred to multiexcitonic triplet pair states. At the same time, negligible spectral changes from time-resolved fluorescence spectra were found, which clearly demonstrates the fluorescence originates solely from the bright S_1 state. Quasi-equilibrium between local excitonic states (S_1) and multiexcitonic triplet pair states (1TT) accounts well for the above experimental findings achieved by biphasic SF.^[65] As biphasic excited-state population shifts to multiexcitonic states and the geometric feature of **QP1** whose each TIPS-pentacene constituent share similar circumstances for SF processes are considered, two possible mechanisms revealed in the solid-state are excluded from interpreting biphasic SF processes in **QP1**. Rather, multiexciton generation via two different channels is suggested as a new possible mechanism in **QP1** combining the results from *fs*-transient absorption and time-resolved fluorescence measurements. Two distinct SF pathways via through-bond and -space interactions will be further discussed in the remaining section based on theoretical calculations.

For **TP2** and **QP2**, SF processes proceed more inefficiently as revealed from *fs*-transient absorption spectra. Contrary to the clear spectral rise of new ESA bands and GSB signals from *fs*-transient absorption spectra of **TP1** and **QP1**, the overall transient absorption signals of **TP2** and **QP2** decay over time. Along with the depletion of S_1 state population, a new ESA band centered around 530 nm emerges, however, a complete spectral evolution

RESEARCH ARTICLE

Table 1. Calculated energy difference between S_1 and 1TT states (ΔE_{SF}), square of non-adiabatic coupling (NAC^2) and multiexciton generation rate (SF rate) in the truncated dimer sets of **TP1**, **QP1** and **HP2** obtained by the restricted active-space configuration interaction method with double spin-flip (RAS-2SF). NAC is defined as $(|y|/\Delta E)$, where $|y|$ is the norm of the one-particle transition density matrix and ΔE is the energy difference between S_1 and 1TT states of uncorrected RAS-2SF energies. SF rate is proportional to $(|y|/\Delta E)^2 \exp(-\alpha\beta\Delta E_{SF})$, where α is set to 0.5 as the original paper which proposed the three-state kinetics model and β is $1/kT$ where k is the Boltzmann constant and T is room temperature of 298K.

		ΔE_{SF} (eV)	NAC^2	SF rate	Contribution of through-space coupling (%)
TP1	1- <i>meta</i>	-0.77	9.9×10^{-6}	3.1×10^1	0.00
	2- <i>meta</i>	-0.77	9.1×10^{-7}	3.1×10^0	0.21
	3- <i>meta</i>	-0.64	7.6×10^{-6}	1.9×10^0	0.05
QP1	1- <i>ortho</i>	-0.78	2.5×10^{-1}	1.0×10^6	0.94
	2- <i>ortho</i>	-0.76	6.7×10^{-4}	1.7×10^3	0.73
	1- <i>meta</i>	-0.71	3.1×10^{-6}	3.2×10^0	0.02
	2- <i>meta</i>	-0.71	9.0×10^{-6}	8.8×10^0	0.01
	1- <i>para</i>	-0.71	1.3×10^{-4}	1.2×10^2	0.00
	2- <i>para</i>	-0.71	2.1×10^{-4}	2.1×10^2	0.00
	HP2	1- <i>ortho</i>	-0.58	7.1×10^{-3}	6.1×10^2
2- <i>ortho</i>		-0.68	2.1×10^{-6}	1.2×10^0	0.00
3- <i>ortho</i>		-0.65	1.8×10^{-5}	5.3×10^0	0.20
4- <i>ortho</i>		-0.61	1.7×10^{-6}	2.5×10^{-1}	0.00
5- <i>ortho</i>		-0.64	1.3×10^{-6}	3.6×10^{-1}	0.00
6- <i>ortho</i>		-0.48	2.1×10^{-4}	2.3×10^0	0.66
1- <i>meta</i>		-0.60	3.0×10^{-8}	3.3×10^{-3}	0.00
2- <i>meta</i>		-0.61	6.5×10^{-8}	8.5×10^{-3}	0.00
3- <i>meta</i>		-0.60	3.0×10^{-8}	3.7×10^{-3}	0.00
4- <i>meta</i>		-0.60	3.0×10^{-8}	3.3×10^{-3}	0.00
5- <i>meta</i>		-0.61	3.0×10^{-8}	4.7×10^{-3}	0.00
6- <i>meta</i>		-0.61	1.2×10^{-7}	1.7×10^{-2}	0.00
1- <i>para</i>		-0.59	7.5×10^{-7}	7.7×10^{-2}	0.00
2- <i>para</i>		-0.64	4.6×10^{-7}	1.1×10^{-1}	0.00
3- <i>para</i>		-0.61	1.7×10^{-6}	1.3×10^{-1}	0.00

was not investigated due to the limited time window of *fs*-transient absorption spectroscopy. Accordingly, randomly interleaved pulse train (RIPT) spectroscopic measurements were performed to monitor excited states of **TP2** and **QP2** over the temporal limit of optical delays and the monitored kinetics are matched well with fluorescence depletion dynamics from TCSPC measurements.^[66] Time constants of 11 and 7 ns were obtained for **TP2** and **QP2**, respectively, from RIPT measurements, which necessarily suggest the existence of an additional non-radiative decay channel when S_1 state lifetime of TIPS-pentacene monomer (~13 ns) is considered.^[67] As chromophores within Type2 dendrimers are more distant compared to those within Type1 dendrimers, it is clearly demonstrated that much weaker couplings are developed for SF processes. Inefficient SF processes for Type2 dendrimers are analogous to those for the *para*-phenylene-bridged pentacene dimer (time constant of 6 ns) whose chromophores are linked by three phenyl linkers.^[44]

For **HP2**, a noticeable spectral evolution was monitored from its transient absorption spectrum (Figure 4). After structural relaxation in the excited state, which commonly occurs in our dendrimers, a distinct peak around 535 nm emerges along with the decay of broad ESA bands of S_1 state at the rate of 40 ps. The peculiar process in the excited-state was further investigated by time-resolved fluorescence measurements. At the rate monitored

from the transient absorption temporal profile, fluorescence intensity slightly decreases over time without any spectral evolution, which demonstrates a bit of bright S_1 state depletes. Since broad and red-shifted fluorescence bands attributed to excimer states do not contribute to the time-resolved fluorescence spectrum, it is suggested that non-fluorescent multiexcitonic triplet pair states are generated.^[67-68] Previously, Yablon et al. described the distinct ESA band located between the broad ESA bands in the transient absorption spectrum of pentacene polymers by the linear combination of transient absorption signals of S_1 and 1TT states.^[69] Similarly, the transient absorption spectrum of the hexamer is well accounted for by the quasi-equilibrium between the two states, however, excited-state populations remain at the S_1 state much dominantly (Figure 4). Since a singlet excitation effectively migrates within the hexamer by Förster energy transfer, a stochastic SF process is suggested at a hot spot of relatively efficient electronic coupling for SF process which is developed by steric effects between bulky TIPS-pentacenes. Afterwards, remaining S_1 state populations are transferred to multiexcitonic triplet pair states at a slower rate of 5.6 ns which is analogous to SF rates in **TP2** and **QP2**. In the later part, the proposed SF process in a hot spot within **HP2** will be investigated by theoretical calculations.

RESEARCH ARTICLE

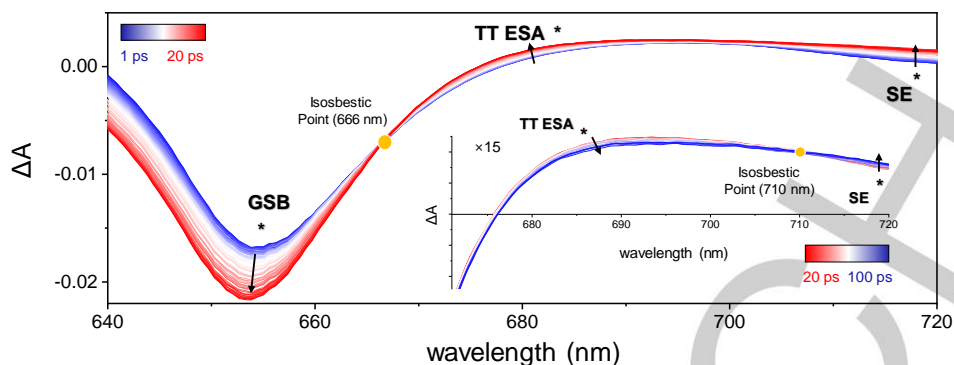


Figure 5. Magnified *fs*-transient absorption spectra of **QP1** in toluene spanning from 640 to 720 nm. Spectral evolution and isosbestic points during biphasic SF processes are described.

Quantum chemical calculations

To evaluate SF dynamics in oligoacene dendrimers observed from time-resolved absorption/fluorescence measurements, quantum chemical calculations were conducted for TIPS-pentacene dendrimers. Possible conformers of TIPS-pentacene dendrimers were carefully investigated. Excitation characters, coupling strengths (non-adiabatic coupling, NAC) between S_1 and ^1TT states, and SF rates (multiexciton generation rates) were calculated by the RAS-2SF method.^[16, 37, 45, 70-72] Since dendrimers studied here are weakly interacting, the optimized structures of trimer, tetramer and hexamer were truncated to sets of dimers for RAS-2SF calculations. Overestimated RAS-2SF energies could be partially refined by adding the difference between RAS-2SF and DFT energies for the same electronic excitation character.^[73] SF rates were calculated based on the three-state model devised by Feng et al. which attempts to obtain a relative rate with respect to a reference system.^[55] Detailed information on quantum chemical calculations is described in SI.

Corrected RAS-2SF excitation energies of S_1 (E_{S_1}) and ^1TT states ($E_{^1\text{TT}}$), energy differences between S_1 and ^1TT states (ΔE_{SF}), square of non-adiabatic coupling strengths (NAC^2), and SF rates of all model dimers derived from the TIPS-pentacene dendrimers are tabulated in Table 1 & S3. First of all, we compared the calculated SF rates of Type1 and Type2 oligomers. As expected from time-resolved measurements, calculated SF rates were much slower for **TP2** and **QP2** compared to those of Type1 counterparts. While the energetics (ΔE_{SF}) are slightly affected by the number of phenyl linkers between chromophores, there are more notable changes in coupling strengths (NAC^2) which are significantly weakened in the dimers truncated from Type2 dendrimers. Even though effects from vibrations and rotational motions of each chromophore within dendrimers were not reflected, large discrepancies between coupling strengths sufficiently account for relatively inefficient SF processes in **TP2** and **QP2** (experimental rates of $\sim 10^9 \text{ s}^{-1}$).

In line with the calculated coupling strengths of **TP2** and **QP2**, all *meta*- and *para*-linked truncated dimer sets of **HP2** exhibit small values. However, it is peculiar to observe a single *ortho*-linked truncated dimer whose coupling strength is significantly high ($\text{NAC}^2 = 7.1 \times 10^{-3}$). Despite a relatively weak energetic driving force ($\Delta E_{\text{SF}} = -0.58 \text{ eV}$) relative to those of **TP1** and **QP1** (ΔE_{SF} ranging from -0.64 to -0.78 eV), the calculated SF rate at the *ortho*-linked SF hot spot in **HP2** (1-*ortho* in Table 1) is comparable

to the second fastest component of the SF pathway ($r \sim 10^3$) in the most efficient SF chromophores among our TIPS-pentacene dendrimers, **QP1**. The SF hot spot in **HP2** originates from its structural heterogeneity due to steric hindrance between six chromophores within the dendrimer. To illustrate the uniqueness of SF hot spot in **HP2**, we compared the 1-*ortho* of **HP2** with 1-*ortho* of **QP2**. As revealed from the minimum-energy structures of **HP2**, a relative orientation between two chromophores at the SF hot spot is close to the π - π slip-stacked structure of 1-*ortho* of **QP2**. However, the distance between the two chromophore at SF hot spot is reduced from 8.8 to 7.1 Å due to tight packing caused by severe crowdedness in **HP2**. A closer proximity between the two chromophores at the SF hot spot developed by steric hindrance strengthens electronic coupling and it compensates for slight energetic disfavor, which enables efficient SF process.

Lastly, coupling strengths in **QP1** were examined. There are clear differences in coupling strengths among *ortho*-, *meta*- and *para*-linkages. In line with the result of **TP1**, coupling through the *meta*-linkage is unfavorable ($\text{NAC}^2 < 1.0 \times 10^{-5}$).^[63] SF processes are expected to be efficient via two SF channels (*ortho*- and *para*-linkages), while there exists a slight difference in the energetic driving force which is greater in *ortho*-linked truncated dimers. This may implicate that multiexcitonic triplets pair generated in *ortho*-linked truncated dimers is relatively stable compared to that in *para*-linked truncated dimers. With the aid of relatively stronger energetic driving force and non-adiabatic coupling, SF rates via *ortho*-linkage were calculated to be faster ($r > 10^3$). To distinguish the effects of through-bond and -space interactions in *ortho*- and *para*-linkages, non-adiabatic coupling strengths were calculated with and without the linkers ($\text{NAC}_{\text{w/L}}$ and $\text{NAC}_{\text{w/o,L}}$, respectively) and the contribution of through-space coupling was evaluated as $(\text{NAC}_{\text{w/o,L}})^2 / (\text{NAC}_{\text{w/L}})^2$.^[55] While through-space interactions are negligible in *para*-linked truncated dimers ($(\text{NAC}_{\text{w/o,L}})^2 / (\text{NAC}_{\text{w/L}})^2 \sim 0$), they play a major role in enhancing electronic coupling in *ortho*-linked truncated dimers ($(\text{NAC}_{\text{w/o,L}})^2 / (\text{NAC}_{\text{w/L}})^2$ of 0.73 and 0.94). Interestingly, when through-space is completely neglected, coupling strengths in both truncated dimers are similar, which suggest *ortho*- and *para*-linkages contribute similarly to the through-bond interactions. These results on **QP1** demonstrate that both channels of through-bond and space operate independently to generate multiexcitonic triplet pairs of different boundness, which is correlated with experimentally observed biphasic SF dynamics.

RESEARCH ARTICLE

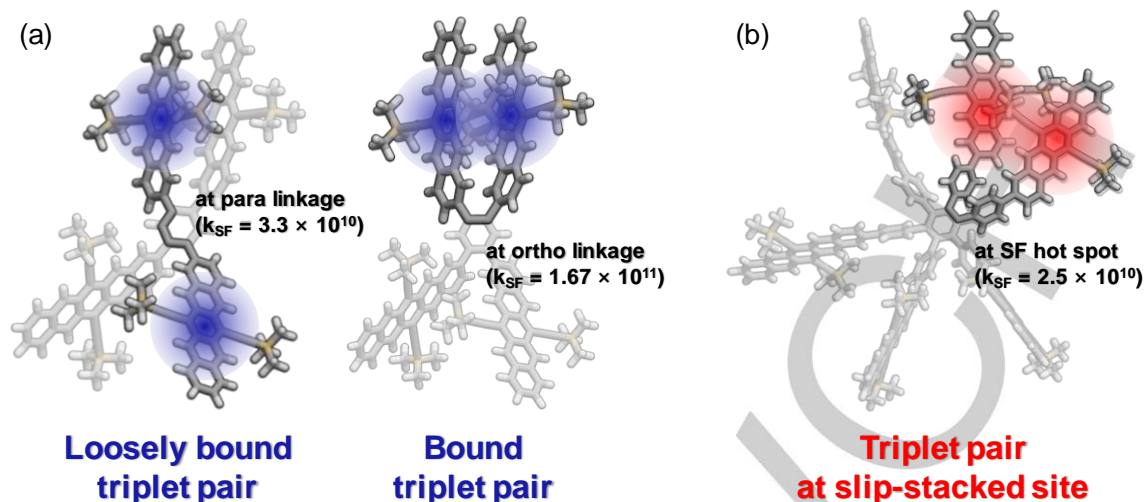


Figure 6. Schematic diagrams for the generation of multiexcitonic triplet pairs in (a) QP1 and (b) HP2.

Multiexcitonic triplet pairs in dendrimers

Finally, multiexcitonic triplet pairs generated in QP1 and HP2 are discussed. Based on the RAS-2SF calculations, SF processes in QP1 occur via two channels, through-space (*ortho*-linkage) and through-bond (*para*-linkage) interactions. As shown in Figure 3, TA spectral evolutions proceed with time constants of 6 and 30 ps. Along with the second time constant (30 ps), ESA band around 520 nm further rises and red-shifts and ESA band around 685 nm slightly decreases (Figure 5). From these spectral evolutions, two multiexcitonic triplet pair states of different boundness are proposed as illustrated in Figure 6. ¹TT states at *ortho*- and *para*-linked chromophores develop at the time constant of 6 and 30 ps via through-space and bond interactions, respectively, which finally reaches thermal equilibrium between the two multiexcitonic triplet pairs. ESA bands for free triplet and multiexcitonic triplet pair have been estimated by Khan et al. based on Pariser-Parr-Pople (PPP) π -electron model.^[74] According to their results, the ESA band in the visible region (500–600 nm) red-shifts for free triplet compared to that of multiexcitonic triplet pair and the ESA band spanning from 700 to 800 nm disappears for free triplet species. In addition, the calculation results show that the intensity of NIR absorption diminishes as the intermolecular interactions are weakened. This calculation result matches well with our demonstration of the generation of a less-bound TT state at *para*-linked chromophores that is based on two spectral features, the red-shift of ESA band around 520 nm and the diminution of ESA band around 700 nm, which arise with the rate constant of 30 ps.

For HP2, as revealed by the RAS-2SF calculation and geometry optimization results, a stochastic SF process is proposed at the hot spot developed by steric hindrance between bulky TIPS-pentacenes. As a slip-stacked geometry is developed and the distance between two TIPS-pentacenes is reduced at the hot spot of HP2, a through-space interaction is enhanced to facilitate SF process ($|NAC|$ of HP2— 8.4×10^{-2} and $|NAC|$ of QP2— 2.1×10^{-3}). The calculation result coincides with the experimental observation of the SF process at the rate of 40 ps in HP2 whose peculiar TA spectrum is described well by the linear combination of TA spectra

of S_1 and T_1 states obtained by *fs*- and *ns*-transient absorption spectroscopies, respectively (Figure 4). The intensity of ESA signal at 570 nm where the ESA signal of triplet species is absent is reduced to one sixth approximately along with the suggested dynamics, which further supports the stochastic SF process within HP2 (Figure S62).

Conclusions

On the basis of time-resolved absorption/fluorescence spectroscopic measurements and quantum chemical calculations, SF processes in TIPS-tetracene/pentacene dendrimers were thoroughly investigated. Experimental results and calculated SF energetics/coupling strengths provide in-depth insights into SF pathways in our dendrimers. From a molecular viewpoint, our oligomerization strategy created multiple channels for the generation of multiexcitonic triplet pairs. In addition, interactions via through-bond and -space were dissected, which provides practical information for designing multichromophoric SF systems. From the viewpoint of structural heterogeneity, the generation of multiexcitonic triplet pairs of different boundness and the SF process at the SF hot spot were proposed as coupling strengths and energetics are sensitive to relative distances and orientations between chromophores. As our dendrimers mimic amorphous solid-states whose SF dynamics proceed in the incoherent coupling regime, we underline the importance of microscopic ordering between SF chromophores to maximize the efficiency of the exciton multiplication process for the application in organic photovoltaic devices.

Acknowledgments

The research at Yonsei University was supported by the NRF (National Research Foundation of Korea) grant funded by Korea government (NRF-2016R1E1A1A01943379). This work was also supported by AFOSR/AOARD grant (FA2386-17-1-4086). The

RESEARCH ARTICLE

research at National University of Singapore was supported by MOE Tier 2 grant (MOE2018-T2-1-152) and Tier 3 programme (MOE2014-T3-1-004). The research at Incheon National University was supported by the NRF grant (NRF-2019R1G1A1099961). Basic Science Research Program through the NRF (NRF2017R1A6A1A06015181) grant funded by the Ministry of Education also supported this work.

Keywords: Oligoacene • Dendrimer • Singlet fission • Time-resolved spectroscopy • Quantum chemical calculation

- [1] M. B. Smith, J. Michl, *Chem. Rev.* **2010**, *110* (11), 6891-6936.
- [2] M. B. Smith, J. Michl, *Annu. Rev. Phys. Chem.* **2013**, *64*, 361-386.
- [3] P. M. Zimmerman, C. B. Musgrave, M. Head-Gordon, *Acc. Chem. Res.* **2013**, *46* (6), 1339-1347.
- [4] J. J. Burdett, C. J. Bardeen, *Acc. Chem. Res.* **2013**, *46* (6), 1312-1320.
- [5] G. B. Piland, J. J. Burdett, R. J. Dillon, C. J. Bardeen, *J. Phys. Chem. Lett.* **2014**, *5* (13), 2312-2319.
- [6] D. Casanova, *Chem. Rev.* **2018**, *118*, 7164-7207.
- [7] H. Kim, P. M. Zimmerman, *Phys. Chem. Chem. Phys.* **2018**, *20*, 30083.
- [8] K. Miyata, F. S. Conrad-Burton, F. L. Geyer, X. Y. Zhu, *Chem. Rev.* **2019**, *119*, 4261-4292.
- [9] S. N. Sanders, A. B. Pun, K. R. Parenti, E. Kumarasamy, L. M. Yablon, M. Y. Sfeir, L. M. Campos, *Chem.* **2019**, *5*, 1988-2005.
- [10] A. J. Musser, J. Clark, *Annu. Rev. Phys. Chem.* **2019**, *70*, 323-351.
- [11] W. Shockley, H. J. Queisser, *J. Appl. Phys.* **1961**, *32*, 510-519.
- [12] M. C. Hanna, A. J. Nozik, *J. Appl. Phys.* **2006**, *100*, 074510.
- [13] M. Einzinger, T. Wu, J. F. Kompalla, H. L. Smith, C. F. Perkinson, L. Nienhaus, S. Wieghold, D. N. Congreve, A. Kahn, M. G. Bawendi, M. A. Baldo, *Nature* **2019**, *571*, 90-94.
- [14] M. J. Y. Tayebjee, A. A. Gray-Weale, T. W. Schmidt, *J. Phys. Chem. Lett.* **2012**, *3* (19), 2749-2754.
- [15] A. Rao, R. H. Friend, *Nat. Rev. Mater.* **2017**, *2*, 17063.
- [16] P. M. Zimmerman, F. Bell, D. Casanova, M. Head-Gordon, *J. Am. Chem. Soc.* **2011**, *133*, 19944-19952.
- [17] S. R. Yost, J. Lee, M. W. B. Wilson, T. Wu, D. P. McMahon, R. R. Parkhurst, N. J. Thompson, D. N. Congreve, A. Rao, K. Johnson, M. Y. Sfeir, M. G. Bawendi, T. M. Swager, R. H. Friend, M. A. Baldo, T. V. Voorhis, *Nat. Chem.* **2014**, *6*, 492-497.
- [18] N. V. Korovina, N. F. Pompetti, J. C. Johnson, *J. Chem. Phys.* **2020**, *152*, 040904.
- [19] W. -L. Chan, M. Ligges, A. Jailaubekov, L. Kaake, L. Miaja-Avila, X. -Y. Zhu, *Science* **2011**, *344* (6062), 840-845.
- [20] W. -L. Chan, M. Ligges, X. -Y. Zhu, *Nat. Chem.* **2012**, *4*, 1541-1545.
- [21] W. -L. Chan, T. C. Berkelbach, M. R. Provorso, N. R. Monahan, J. R. Tritsch, M. S. Hybertsen, D. R. Reichman, J. Gao, X. -Y. Zhu, *Acc. Chem. Res.* **2013**, *46* (6), 1321-1329.
- [22] P. M. Zimmerman, Z. Zhang, C. B. Musgrave, *Nat. Chem.* **2010**, *2*, 648-652.
- [23] D. Beljonne, H. Yamagata, J. L. Bredas, F. C. Spano, Y. Olivier, *Phys. Rev. Lett.* **2013**, *110*, 226402.
- [24] A. J. Musser, M. Liebel, C. Schnedermann, T. Wende, T. B. Kehoe, A. Rao, P. Kukura, *Nat. Phys.* **2015**, *11*, 352-357.
- [25] R. D. Pensack, A. J. Tilley, S. R. Parkin, T. S. Lee, M. M. Payne, D. Gao, A. A. Jahnke, D. G. Oblinsky, P. -F. Li, J. E. Anthony, D. S. Seferos, G. A. Scholes, *J. Am. Chem. Soc.* **2015**, *137*, 6790-6803.
- [26] A. A. Bakulin, S. E. Morgan, T. B. Khoe, M. W. B. Wilson, A. W. Chin, D. Zigmantas, D. Egorova, A. Rao, *Nat. Chem.* **2016**, *8*, 16-23.
- [27] S. Lukman, J. M. Hodgkiss, D. H. P. Turban, N. D. M. Hine, S. Dong, J. Wu, N. C. Greenham, A. J. Musser, *Nat. Commun.* **2016**, *7*, 1-13.
- [28] E. G. Fuemmeler, S. N. Sanders, A. B. Pun, E. Kumarasamy, T. Zeng, K. Miyata, M. L. Steigerwald, X. -Y. Zhu, M. Y. Sfeir, L. M. Campos, N. Ananth, *ACS. Cent. Sci.* **2016**, *2*, 316-324.
- [29] A. F. Morrison, J. M. Herbert, *J. Phys. Chem. Lett.* **2017**, *8*, 1442-1448.
- [30] N. R. Monahan, D. Sun, H. Tamura, K. W. Williams, B. Xu, Y. Zhong, B. Kumar, C. Nuckolls, A. R. Harutyunyan, G. Chen, H. -L. Dai, D. Beljonne, Y. Rao, X. -Y. Zhu, *Nat. Chem.* **2017**, *9*, 341-346.
- [31] K. Miyata, Y. Kurashige, K. Watanabe, T. Sugimoto, S. Takahashi, S. Tanaka, J. Takeya, T. Yanai, Y. Matsumoto, *Nat. Chem.* **2017**, *9*, 983-989.
- [32] H. L. Stern, A. Cheminal, S. R. Yost, K. Broch, S. L. Bayliss, K. Chen, M. Tabachnyk, K. Thorley, N. Greenham, J. M. Hodgkiss, J. Anthony, M. Head-Gordon, A. J. Musser, A. Rao, R. H. Friend, *Nat. Chem.* **2017**, *9*, 1205-1211.
- [33] S. M. Hart, W. R. Silva, R. R. Frontiera, *Chem. Sci.* **2018**, *9*, 1242-1250.
- [34] K. Broch, J. Dieterle, F. Branchi, N. J. Hestand, Y. Olivier, H. Tamura, C. Cruz, V. M. Nichols, A. Hinderhofer, D. Beljonne, F. C. Spano, G. Cerullo, C. J. Bardeen, F. Schreiber, *Nat. Commun.* **2018**, *9*, 954.
- [35] A. M. Alvertis, S. Lukman, T. J. H. Hele, E. G. Fuemmeler, J. Feng, J. Wu, N. C. Greenham, A. W. Chin, A. J. Musser, *J. Am. Chem. Soc.* **2019**, *141* (44), 17558-17570.
- [36] V. Jankus, E. W. Snedden, D. W. Bright, E. Arac, D. Dai, A. P. Monkman, *Phys. Rev. B* **2013**, *87*, 224202.
- [37] X. Feng, A. B. Kolomeisky, A. I. Krylov, *J. Phys. Chem. C* **2014**, *118* (34), 19608-19617.
- [38] P. I. Dron, J. Michl, J. C. Johnson, *J. Phys. Chem. A* **2017**, *121* (45), 8596-8603.
- [39] D. M. Finton, E. A. Wolf, V. S. Zoutenbier, K. A. Ward, I. Biaggio, *AIP Adv.* **2019**, *9*, 095027.
- [40] S. Takahashi, K. Watanabe, Y. Matsumoto, *J. Chem. Phys.* **2019**, *151*, 074703.
- [41] H. Huang, G. He, K. Xu, Q. Wu, D. Wu, M. Y. Sfeir, J. Xia, *Chem.* **2019**, *5*, 2405.
- [42] J. Zirzmeier, D. Lehnher, P. B. Coto, E. T. Chernick, R. Casillas, B. S. Basel, M. Thoss, R. R. Tykwinski, D. M. Guldi, *Proc. Natl. Acad. Sci. U.S.A.* **2015**, *112*, 5325.
- [43] A. M. Muller, Y. S. Avlasevich, W. W. Schoeller, K. Mullen, C. J. Bardeen, *J. Am. Chem. Soc.* **2007**, *129*, 14240-14250.
- [44] S. N. Sanders, E. Kumarasamy, A. B. Pun, M. T. Trinh, B. Choi, J. Xia, E. J. Tafflet, J. Z. Low, J. R. Miller, X. Roy, X. -Y. Zhu, M. L. Steigerwald, M. Y. Sfeir, L. M. Campos, *J. Am. Chem. Soc.* **2015**, *137*, 8965-8972.
- [45] N. V. Korovina, S. Das, Z. Nett, X. Feng, J. Joy, R. Haiges, A. I. Krylov, S. E. Bradforth, M. E. Thompson, *J. Am. Chem. Soc.* **2016**, *120*, 4473-4481.
- [46] J. D. Cook, T. J. Carey, N. H. Damrauer, *J. Phys. Chem. A* **2016**, *6*, 451-456.
- [47] E. Kumarasamy, S. N. Sander, M. J. Y. Tayebjee, A. Asadpoordarvish, T. J. H. Hele, E. G. Fuemmeler, A. B. Pun, L. M. Yablon, J. Z. Low, D. W. Paley, J. C. Dean, B. Choi, G. D. Scholes, M. L. Steigerwald, N. Ananth, D. R. McCamey, M. Y. Sfeir, L. M. Campos, *J. Am. Chem. Soc.* **2017**, *139*, 12488-12494.
- [48] B. S. Basel, J. Zirzmeier, C. Hetzer, B. T. Phelan, M. D. Krzyaniak, S. R. Reddy, P. B. Coto, N. E. Horwitz, R. M. Young, F. J. White, F. Hampel, T. Clark, M. Thoss, R. R. Tykwinski, M. R. Wasielewski, D. M. Guldi, *Nat. Commun.* **2017**, *8*, 15171.
- [49] N. V. Korovina, J. Joy, X. Feng, C. Feltenberger, A. I. Krylov, S. E. Bradforth, M. E. Thompson, *J. Am. Chem. Soc.* **2018**, *140*, 10179-10190.
- [50] B. S. Basel, J. Zirzmeier, C. Hetzer, S. R. Reddy, B. T. Phelan, M. D. Krzyaniak, M. K. Volland, P. B. Coto, R. M. Young, T. Clark, M. Thoss, R. R. Tykwinski, M. R. Wasielewski, D. M. Guldi, *Chem.* **2018**, *4*, 1092-1111.
- [51] B. S. Basel, C. Hetzer, J. Zirzmeier, D. Thiel, R. Guldi, F. Hampel, A. Kahnt, T. Clark, D. M. Guldi, R. R. Tykwinski, *Chem. Sci.* **2019**, *10*, 3854-3863.
- [52] I. Papadopoulos, J. Zirzmeier, C. Hetzer, Y. J. Bae, M. D. Krzyaniak, M. M. R. Wasielewski, T. Clark, R. R. Tykwinski, D. M. Guldi, *J. Am. Chem. Soc.* **2019**, *141*, 6191-6203.
- [53] S. N. Sanders, E. Kumarasamy, K. J. Fallon, M. Y. Sfeir, L. M. Campos, *Chem. Sci.* **2020**, *11*, 1079-1084.

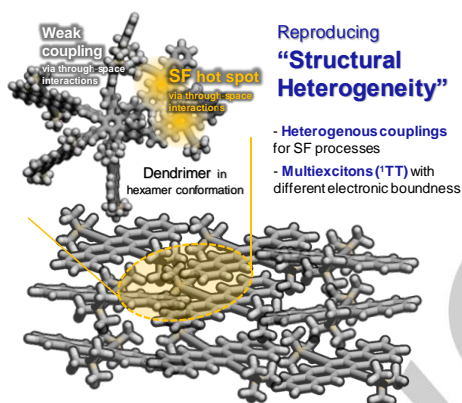
RESEARCH ARTICLE

- [54] X. Feng, D. Casanova, A. I. Krylov, *J. Phys. Chem. C* **2016**, *120*, 19070-19077.
- [55] X. Feng, A. I. Krylov, *Phys. Chem. Chem. Phys.* **2016**, *18*, 7751-7761.
- [56] S. Ito, T. Nagami, M. Nakano, *J. Phys. Chem. A* **2016**, *120*, 6236-6241.
- [57] H. Nagashima, S. Kawaoka, S. Akimoto, T. Tachikawa, Y. Matsui, H. Ikeda, Y. Kobori, *J. Phys. Chem. Lett.* **2018**, *9*, 5855-5861.
- [58] H. Yamagata, J. Norton, E. Hontz, Y. Olivier, D. Beljonne, J. L. Bredas, R. J. Silbey, F. C. Spano, *J. Chem. Phys.* **2011**, *134*, 204703.
- [59] N. J. Hestand, H. Yamagata, B. Xu, D. Sun, Y. Zhong, A. R. Harutyunyan, G. Chen, H. -L. Dai, Y. Rao, F. C. Spano, *J. Phys. Chem. C* **2015**, *119*, 22137-22147.
- [60] N. Monahan, X. -Y. Zhu, *Annu. Rev. Phys. Chem.* **2015**, *66*, 601-618.
- [61] C. Hetzer, B. S. Basel, S. M. Kopp, F. Hampel, F. J. White, T. Clark, D. M. Guldi, R. R. Tykwinski, *Angew. Chem. Int. Ed.* **2019**, *58*, 15263-15267.
- [62] Y. Hong, J. Kim, W. Kim, C. Kaufmann, H. Kim, F. Wurthner, D. Kim, *J. Am. Chem. Soc.* **2020**, *142* (17), 7845-7857.
- [63] K. Shizu, C. Adachi, H. Kaji, *J. Phys. Chem. A* **2020**, *124*, 3641-3651.
- [64] T. S. Lee, Y. L. Lin, H. Kim, R. D. Pensack, B. P. Rand, G. D. Scholes, *J. Phys. Chem. Lett.* **2018**, *9*, 4087-4095.
- [65] A. T. Gilligan, E. G. Miller, T. Sammakia, N. H. Damrauer, *J. Am. Chem. Soc.* **2019**, *141* (14), 5961-5971.
- [66] T. Nakagawa, K. Okamoto, H. Hanada, R. Katoh, *Opt. Lett.* **2016**, *41* (7), 1498-1501.
- [67] B. J. Walker, A. J. Musser, D. Beljonne, R. H. Friend, *Nat. Chem.* **2013**, *5*, 1019-1024.
- [68] C. B. Dover, J. K. Gallaher, L. Frazer, P. C. Tapping, A. J. Petty II, M. J. Crossley, J. E. Anthony, T. W. Kee, T. W. Schmidt, *Nat. Chem.* **2018**, *10*, 305-310.
- [69] L. M. Yablun, S. N. Sanders, H. Li, K. R. Parenti, E. Kumarasamy, K. J. Fallon, M. J. A. Hore, A. Cacciuto, M. Y. Sfeir, L. M. Campos, *J. Am. Chem. Soc.* **2019**, *141*, 9564-9569.
- [70] X. Feng, A. V. Luzanov, A. I. Krylov, *J. Phys. Chem. Lett.* **2013**, *4*, 3845.
- [71] D. Casanova, *J. Chem. Theory Comput.* **2015**, *10*, 324.
- [72] D. Casanova, A. I. Krylov, *Phys. Chem. Chem. Phys.* **2020**, *22*, 4326.
- [73] M. H. Farag, A. I. Krylov, *J. Phys. Chem. C* **2018**, *122*, 25753.
- [74] S. Khan, S. Mazumdar, *J. Phys. Chem. Lett.* **2017**, *8*, 5943-5948.
- [75] J. J. Snellenburg, S. P. Laptinok, R. Seger, K. M. Mullen, I. H. M. Stokkum, *J. Stat. Softw.* **2012**, *49*, 1.

RESEARCH ARTICLE

RESEARCH ARTICLE

Heterogeneous couplings and energetics for SF process were developed in dendritic structures which mimic complicated SF dynamics in amorphous solids. SF in dendritic structures was thoroughly investigated by time-resolved spectroscopic techniques and quantum chemical calculations in respect of relative orientation/distance between chromophores and through-bond/-space interactions.



J. Kim, H. T. Teo, Y. Hong, Dr. J. Oh, Prof. H. Kim*, Prof. C. Chi* and Prof. D. Kim*

Page No. – Page No.

Multiecitonic Triplet Pair Generation in Oligoacene Dendrimers as Amorphous Solid-state Miniatures

Accepted Manuscript